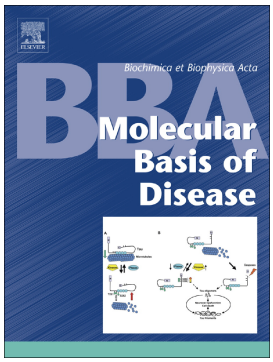

Glutaredoxin-2 and Sirtuin-3 deficiencies impair cardiac mitochondrial energetics but their effects are not additive

Neoma T. Boardman, Baher Migally, Chantal Pileggi, Gaganvir S. Parmar, Jian Ying Xuan, Keir Menzies, Mary-Ellen Harper

PII: S0925-4439(20)30330-6

DOI: https://doi.org/10.1016/j.bbadis.2020.165982

Reference: BBADIS 165982

To appear in: *BBA - Molecular Basis of Disease*

Received date: 14 May 2020

Revised date: 6 September 2020

Accepted date: 24 September 2020

Please cite this article as: N.T. Boardman, B. Migally, C. Pileggi, et al., Glutaredoxin-2 and Sirtuin-3 deficiencies impair cardiac mitochondrial energetics but their effects are not additive, *BBA - Molecular Basis of Disease* (2020), https://doi.org/10.1016/j.bbadis.2020.165982

Glutaredoxin-2 and Sirtuin-3 deficiencies impair cardiac mitochondrial energetics but their effects are not additive

Neoma T Boardman[1,2], Baher Migally[1], Chantal Pileggi[1], Gaganvir S Parmar[1], Jian Ying Xuan[1], Keir Menzies[1,3], and Mary-Ellen Harper[1,*]

1. Department of Biochemistry, Microbiology and Immunology, and Ottawa Institute of Systems Biology, Faculty of Medicine, University of Ottawa, Ottawa, ON, Canada
2. Department of Medical Biology, Faculty of Health Sciences, UiT-Arctic University of Norway, Tromsø, Norway
3. Interdisciplinary School of Health Sciences, Faculty of Health Sciences, University of Ottawa, Ottawa, ON, Canada

*** Corresponding author:** Dr. M-E Harper, Department of Biochemistry Microbiology and Immunology; Faculty of Medicine; University of Ottawa; 451 Smyth Rd.; Ottawa ON; Canada K1H 8M5. mharper@uottawa.ca

Running title: Combined GRX2 and SIRT3 deficiency impairs cardiac mitochondrial function

Keywords: mitochondria, oxidative phosphorylation, reactive oxygen species, oxidative stress, glutathione, redox, fibrosis, hypertrophy

Highlights

- GRX2 and SIRT3 are important in the control of oxidative stress and mitochondrial function in the heart
- The absence of both GRX2 and SIRT3 impairs overall mitochondrial respiratory capacity
- In human left ventricle tissue, expression of GRX2 and SIRT3 is positively correlated

Abstract

Altered redox biology and oxidative stress have been implicated in the progression of heart failure. Glutaredoxin-2 (GRX2) is a glutathione-dependent oxidoreductase and catalyzes the reversible deglutathionylation of mitochondrial proteins. Sirtuin-3 (SIRT3) is a class III histone deacetylase and regulates lysine acetylation in mitochondria. Both GRX2 and SIRT3 are considered as key in the protection against oxidative damage in the myocardium. Knockout of either contributes to adverse heart pathologies including hypertrophy, hypertension, and cardiac dysfunction. Here, we created and characterized a GRX2 and SIRT3 double-knockout mouse model, hypothesizing that their deletions would have an additive effect on oxidative stress, and exacerbate mitochondrial function and myocardial structural remodeling. Wildtype, single-gene knockout (*Sirt3*$^{-/-}$, *Grx2*$^{-/-}$), and double-knockout mice (*Grx2*$^{-/-}$/*Sirt3*$^{-/-}$) were compared in heart weight, histology, mitochondrial respiration and H_2O_2 production. Overall, the hearts from *Grx2*$^{-/-}$/*Sirt3*$^{-/-}$ mice displayed increased fibrosis and hypertrophy versus wildtype. In the *Grx2*$^{-/-}$ and the *Sirt3*$^{-/-}$ we observed changes in mitochondrial oxidative capacity, however this was associated with elevated H_2O_2 emission only in the *Sirt3*$^{-/-}$. Similar changes were observed but not worsened in hearts from *Grx2*$^{-/-}$/*Sirt3*$^{-/-}$ mice, suggesting that these changes were not additive. In human myocardium, using genetic and histopathological data from the human Genotype-Tissue Expression consortium, we confirmed that SIRT3 expression correlates inversely with heart pathology. Altogether, GRX2 and SIRT3 are important in the control of cardiac mitochondrial redox and oxidative processes, but their combined absence does not exacerbate effects, consistent with the overall conclusion that they function together in the complex redox and antioxidant systems in the heart.

1. Introduction

Cardiac myocyte energy demands are continuously high on account of the contractile activities of the heart. To meet the associated demands for ATP, cardiac myocytes rely on the β-oxidation of fatty acids in mitochondria. It is estimated that 60-90% of cardiomyocyte ATP demands are met through this pathway, which ultimately fuels the ATP-generating oxidative phosphorylation (OXPHOS) system [30]. OXPHOS includes the mitochondrial electron transport system (ETS) and ATP synthase, and is driven by reducing equivalents (electrons) emanating from substrate oxidations, such as β-oxidation. While mitochondria are the major source (roughly 90%) of cellular ATP in most cell types of the body, they are also important generators of reactive oxygen species (ROS), including superoxide ($O_2^{\cdot-}$), hydrogen peroxide (H_2O_2) and the hydroxyl radical ($^{\cdot}OH$) [5, 41]. The overall levels of ROS are normally kept in balance to minimize oxidative stress while enabling the important roles played by ROS as signaling molecules in many physiological processes [47, 50]. ROS are important messengers in the regulation of cell metabolism and physiological homeostasis, but excessive levels cause oxidative damage and potentially cell death through processes including apoptosis, ferroptosis and necrosis [11, 66, 67]. As such, and given the high rates of substrate oxidation in the myocardium, the heart requires a battery of complex, coordinated systems that counter-balance transient increases in redox and ROS during changes in workload, substrate supply, and energy demand. In the absence of these systems, myocyte oxidative stress, and damage ensue, which are known to be important in the development of cardiac dysfunction in heart failure and in other cardiac diseases [39, 43].

Overall levels of myocardial ATP production by OXPHOS is achieved through multiple mechanisms, including alterations in mitochondriogenesis, mitochondrial dynamics, electron transport system supercomplexes, expression of enzymes involved in fuel oxidation, and protein post-translational modifications (PTMs) [21, 23, 52, 57]. PTMs can acutely control protein function as well as protein-protein interactions, and thereby modulate ROS and the flux though mitochondrial oxidative pathways [20, 40]. The dysregulation of PTMs in mitochondria can result in mitochondrial dysfunction in heart disease [49]. Various PTMs identified in the failing heart have been associated with diminished mitochondrial respiratory capacity, ATP production efficiency, lower antioxidant capacities and associated higher levels of ROS production [12, 53, 58] and lack of metabolic flexibility [59].

In this study, we focus on two proteins responsible for regulating two distinct types of PTM that have been shown to be altered in heart failure and that are known modulators of mitochondrial function: glutaredoxin-2 (GRX2) and sirtuin-3 (SIRT3). These proteins function in reversible deglutathionylation and deacetylation processes, respectively. Protein S-glutathionylation reactions have emerged as key in the control of redox homeostasis [18, 29], ROS levels and protein function [16, 36, 64] in mitochondria. GRX2, predominantly localized in the mitochondria and nuclei of cells, is an oxidoreductase that catalyzes the reversible deglutathionylation of mitochondrial proteins in response to a wide range of GSH/GSSG ratios [6], and may protect the heart from damage due to oxidative stress [7, 64]. Detrimental effects of impaired GRX2-mediated redox signaling are evident in cardiac muscle [7, 34], due likely in large part to the high content of mitochondrial OXPHOS proteins and the central role of mitochondria in meeting cardiac energy demands. GRX2 is reported to target many mitochondrial proteins including cytochrome *c* [14, 18] and uncoupling protein-3 [33]. Importantly, GRX2 also targets complex I (CI) of the ETS, which can alter CI activity and modulate CI ROS release [6, 61]. In line with this, the reversal of a disordered redox environment in which deglutathionylated states of proteins were favoured, resulted in the recovery of CI activity and ATP output [34]. GRX2 has also been shown to control apoptotic signaling factors [64], and thus may be vital for cell survival under oxidative stress conditions, such as in myocardial infarction [7, 64]. In line with this, it is not surprising that low expression of GRX2 expression in human myocardium and that knockout of *Grx2* in mice are associated with the development of heart pathologies including fibrosis, hypertrophy, infarct and hypertension [24, 34, 36].

Reversible lysine acetylation is another type of PTM affecting mitochondrial proteins involved in controlling energy metabolism processes, including fatty acid metabolism, TCA cycle, ETS and OXPHOS. The Sirtuin (SIRT) NAD+ dependent class II histone deacetylase proteins control protein deacetylation and have different subcellular localizations (*i.e.,* nucleus, cytoplasm, mitochondria), different types of PTMs (*e.g.,* acetylation, acylation, succinylation, ADP-ribosylation) and substrate affinities (*e.g.,* acetyl CoA, malonyl co-A, succinate, glutaryl CoA) [45]. Like GRX2, SIRT3 is located in the nucleus and mitochondria, but it controls metabolism through deacetylation (rather than glutathionylation) of key proteins involved in substrate uptake and oxidation pathways, including β-oxidation of fatty acids [19, 48]. Acetylation PTMs have been shown to control myocardial fatty acid oxidation [15]. However, whether SIRT3 increases [3, 56] or inhibits

[27] β-oxidation of fatty acids in the heart remains to be fully elucidated. Downregulated expression of SIRT3 in the heart has also been shown to contribute to pathological metabolic remodeling in heart failure [25, 27, 53]. Recent *in vitro* and *in situ* studies have suggested that through the dynamic association between SIRT3 and ATP synthase, SIRT3 can modulate ATP production [63], and this may also be the case in the heart [2, 27]. Moreover, SIRT3 may control mitochondrial ROS production and preserve antioxidant defenses [53, 63]. Of note, the beneficial effects of SIRT3 in the context of left ventricular hypertrophy, cardiomyopathy, and oxidative stress have been shown through overexpression in mouse models [27].

In the present study, we aimed to assess the impact of knocking out both GRX2 and SIRT3, hypothesizing that the absence of both proteins would lead to exacerbated states of oxidative stress, mitochondrial energetics, oxidative stress, cardiac hypertrophy and fibrosis in *Grx2*$^{-/-}$/*Sirt3*$^{-/-}$ mice compared to single knockouts (*Grx2*$^{-/-}$ or *Sirt3*$^{-/-}$) and to wild type mice.

2. Experimental procedures

2.1 Animals and genotyping

All procedures involving mice were approved by the Animal Care Committee of the University of Ottawa, and done in accordance with the principles and guidelines of the Canadian Council of Animal Care. The 3 R's (Replacement, Reduction, and Refinement) have specifically been addressed when designing the study. Mice were housed in the animal care unit at room temperature (~23 °C) with a 12 h dark/12 h light cycle (lights on at 0700 h), and given free access to a standard rodent chow (44.2% carbohydrates, 6.2% fat, and 18.6% crude protein; diet T.2018, Harlan Teklad, Indianapolis IN) and water. In this study, C57BL/6N GRX2 whole-body knockout (*Grx2* $^{-/-}$) mice were originally obtained from Dr. Marjorie Lou, at the University of Nebraska-Lincoln. C57BL/6N male, wild-type mice were obtained from Charles River Laboratories. 129/Sv SIRT3 whole-body knockout (*Sirt3* $^{-/-}$) and wild-type mice were obtained from JAX®. Whole-body double knockouts of *GRX2* and *Sirt3* (*Grx2*$^{-/-}$/*Sirt3*$^{-/-}$) and matching mixed-background "double wild-types" were produced by crossing the *Grx2* $^{-/-}$ and *Sirt3* $^{-/-}$ mice. Genotyping was confirmed by PCR. Cardiac hypertrophy (heart weight) and fibrosis were assessed in male and female mice; however, there were no genotype-specific differences detected in female mice at 10-12

weeks of age. Thus, for the remaining portion of this study, only male mice (10-12 weeks) were included.

2.2 Determination of cardiac fibrosis

Mouse hearts were immediately dissected and weighed following euthanasia. First, the heart was divided laterally in half across the horizontal midsection. The top portion was placed in 10% formalin and then in 70% ethanol prior to paraffin embedding and used for histological analysis. At the vertical midpoint, 4 µm transverse sections were obtained and stained with Sirius Red, to stain Type 1 and Type 3 collagen fibers. Fibrosis was assessed using Aperio® ImageScope software (Leica Biosystems) in which stained fibers were quantified and normalized to tissue area. Cardiac tissue area was selected, while blood vessels were deselected. An algorithm was then used to quantify pixels with a hue value between 0.88-0.90 (which corresponds to the color of Sirius Red staining) as "positive", while all other non-white pixels are quantified as "negative." The number of positive pixels was then divided by total pixels counted (positive + negative) to give a "% staining" value used to assess fibrosis.

2.3 High resolution respirometry and H_2O_2 production in cardiac myofibers

The Oxygraph-2k (O2k, OROBOROS Instruments, Innsbruck, Austria) was used for measurements of respiration and combined with the Fluorescence-Sensor Green of the O2k-Fluo LED2-Module for H_2O_2 measurement. Hearts from mice (10-12 weeks) were excised and a sample from the apex (~ 50 mg) was taken and split vertically in half. For high resolution respirometry and H_2O_2 analyses, one half of the apex was immediately placed in ice-cold BIOPS buffer containing (mM): CaK_2EGTA 2.77; K_2EGTA 7.23; Na_2ATP 5.77; $MgCl_2*6H_2O$ 6.56, taurine 20; Na^{2+}2-phosphocreatine 15; imidazole 20; DTT 0.5; MES 50; pH 7.1 at 0°C. The other half of the apex was flash-frozen in liquid nitrogen for later enzyme activity assays.

Heart fibers were prepared and permeabilized as previously described [24]. Briefly, this included mechanical teasing, and incubation in 50 µg/mL of saponin in BIOPS for 30 minutes at 4°C, with gentle agitation. Permeabilized fibers were then washed three times in MiR05 buffer containing (mM): EGTA 0.5; $MgCl_2*6H_2O$ 3; lactobionic acid 60; taurine 20, K_2HPO_4 10; HEPES 20; D-sucrose 110; and BSA (albumin) 1g/L; pH 7.1 at 37°C. Fibers were weighed and used immediately for simultaneous determinations of oxygen consumption and H_2O_2 emission using the O2K-Fluorometer. Experiments were conducted

in duplicate chambers, each chamber containing 2 mL Mir05 (37°C) with oxygen concentrations maintained within a narrow range to prevent hypoxia within the sample. Mass-specific oxygen consumption and H_2O_2 flux were calculated using the DatLab 6.0 software (OROBOROS Instruments, Austria). H_2O_2 flux was determined, as previously described, in the presence of 10 µM Amplex UltraRed, 1 U/mL horseradish peroxidase (HRP) and 5 U/mL superoxide dismutase (SOD), with three titrations of 0.1 µM of H_2O_2 to calibrate the fluorimeter [35]. Oxidative stress was characterized by the H_2O_2 production rate/O_2 consumption, as these were measured in parallel.

Complex I-associated proton leak (CI-Leak) was assessed in the presence of malate (2 mM), pyruvate (5 mM) and glutamate (10 mM). Adenosine diphosphate (ADP) (5mM) and Mg^{2+} (5 mM) were subsequently added to quantify Complex I-associated coupled respiration (CI- OXPHOS). To assess maximal OXPHOS capacity (CI&II-associated coupled respiration), succinate (10mM) was added. Phosphorylating respiration was inhibited following the addition of the F_0F_1-ATPase inhibitor, oligomycin (2 µg/mL) (CI+CII-Leak). Antimycin A (2.5 µM; a CIII inhibitor) was added to determine non-mitochondrial (residual) oxygen consumption (ROX). All respiration values were corrected for ROX during analyses. Finally, N,N,N′,N′-tetramethyl-p-phenylenediamine (TMPD) (0.5 mM) and ascorbate (2 mM) were added to evaluate CIV activity, corrected to sodium azide (15 mM). OXPHOS coupling efficiency was calculated as 1-(CI leak/OXPHOS). Values of mitochondrial respiration were expressed as µmol O_2/s/mg wet wt.

The abundance of mitochondria within the tissue was measured by citrate synthase (CS) activity, as previously described [51]. Assays were performed using the BioTek Synergy Mx Microplate Reader at 25°C in 50 mM Tris-HCl (pH 8.0), with 0.2 mM DTNB, 0.1 mM acetyl-CoA and 0.25 mM oxaloacetate. Rate of absorbance change at 412nm and path-length of each well was determined using the BioTek Gen5 Software (BioTek Instruments, Inc., Winooski, VT, USA). Enzyme activity was calculated using the extinction coefficient of $13.6 mM^{-1}cm^{-1}$.

2.4 Protein extraction and quantification

Tissue (from flash frozen samples) was weighed and homogenized in ice-cold RIPA buffer containing (mM): 10 Tris-Cl (pH 8), 1 EDTA, 0.5 EGTA, 140 $NaCl_2$; as well as 1% Triton X-100, 0.1% sodium deoxycholate, 0.1% SDS, and 0.001% protease (P8340 Sigma) and

phosphatase (P5726 Sigma) inhibitors. Samples were homogenized using the Fisherbrand Bead Mill Homogenizer, and then rotated for 1 hour at 4°C, followed by centrifugation at 14,000g for 10 minutes. The pellet was discarded. Protein concentration was determined using a bicinchoninic acid (BCA) (Thermo Fisher Scientific #23225, Rockford, IL) protein assay in a BioTek Synergy Mx Microplate Reader.

2.5 Cardiac GSH and GSSG determinations

Concentrations of GSH and GSSG were determined by HPLC using an Agilent 1100 Series instrument, equipped with a Pursuit 5 C_{18} column operating at a flow rate set to 1mL/min as previously described [24]. The mobile phase consisted of 10% HPLC-grade methanol (HPLC plus, Sigma, 646377), 90% ddH_2O, 0.09% trifluoroacetic acid (Sigma, 302031). In brief, frozen tissues were weighed and homogenized using a bead mill homogeniser (Fisherbrand Bead Mill 24 Homogenizer) in ice-cold 1:1 buffer [1% (v/v) trifluoroacetic acid (Sigma, 302031) and 1% (w/v) meta-phosphoric acid (Sigma, 239275) solution in mobile phase and homogenization buffer (for 25 mL, 250mM sucrose, 10mM TRIS, 3mM EDTA dissolved in mobile phase, pH of 7.4) final pH of 1:1 buffer <1.0] and incubated on ice for 20 minutes. Homogenates were centrifuged at 14,000g for 20 minutes at 4°C. The supernatant was collected for immediate analysis. Retention times for GSH and GSSG were detected using the Agilent UV-visible wavelength detector at 215nm and confirmed with standards using 0.1mM, 0.01mM and 0.001mM of GSH (Sigma, G4251) and GSSG (Sigma, G4501) dissolved in 1:1 buffer. Absolute amounts of GSH and GSSG were determined by integrating the area under the corresponding peaks using the Agilent Chemstation Software and values were calculated from standard curves.

2.5 Immunoblotting

Western blots were performed to assess overall levels of protein glutathionylation. Protein aliquots were suspended in Laemmli buffer (10% glycerol, 2% SDS, 0.0025% bromophenol blue, 62.5 mM Tris-HCl (pH 6.8)) and heated at 95^{o}C for 5 min before separation by SDS/PAGE. Samples prepared in Laemmli buffer with 2% (v/v) b-mercaptoethanol (BME) served as negative controls. BME is a reducing agent and removes glutathionyl moieties from protein cysteine thiols. Samples were electrophoresed on 8% gels and proteins were then transferred to nitrocellulose membranes and blocked in 5% BSA/skim milk powder for 1 hour at room temperature. Western blots to assess global acetylation and SIRT3 levels were also performed. Protein aliquots were suspended in

Laemmli buffer containing 0.1% dithiothreitol (DTT) and electrophoresed on 12% SDS gels. All primary antibodies (PSSG antiserum (1:500, Virogen); anti-SIRT3 (1:1500, Cell Signaling, #549OS); anti-acetylated lysine (1:3000, Thermo Scientific); anti-SOD-1 and SOD-2 (1:2000, Santa Cruz); anti-GRX2 (1:1000, Abcam); anti-GPX4 (1:2000, Abcam); Total OXPHOS Rodent WB Antibody Cocktail (1:2000, Abcam) were incubated overnight at 4°C followed by a 2 hour incubation at room temperature with the appropriate horseradish peroxidase-conjugated secondary antibody (1:5000). Ponceau S staining of membranes as well as Tubulin (1:10000, Sigma) served as loading controls. Protein bands were visualised using Enhanced Chemiluminescent substrate kits (Thermo Scientific) and immunoreactive bands were imaged with the ChemiDoc™ MP Imaging System (Bio-Rad). Bands were quantified using FiJi Software (NIH).

2.6 Identifying transcript correlations from GTEx human tissue data sets

Human heart left ventricle microarray data (Genotype-Tissue Expression (GTEx) project) v5 Human Heart - Left Ventricle RefSeq dataset) were retrieved from the GeneNetwork program as RPKM (Reads Per Kilobase of transcript per Million mapped reads) log2 values and analyzed for correlations between GRX2 (GLRX2) and SIRT3 transcript expression levels. Levels were also correlated to SOD1 and SOD2 expression levels in the same dataset. Raw microarray data are publicly available on the GeneNetwork (www.genenetwork.org) and on Gene Expression Omnibus (https://www.ncbi.nlm.nih.gov/geo/) with the accession number GSE45878 (GTEx, 2015).

2.7 Identifying human data correlations between SIRT3 expression and incidence of adverse heart pathology

SIRT3 transcript expression data from the human GTEx left ventricle dataset were downloaded from the GeneNetwork program as RPKM log2 values, then grouped into high and low SIRT3 transcript expression (the 50 highest and the 50 lowest of the total N). Corresponding pathologists' notes for all 50 GTEx samples in the high or low SIRT3 expression groups were exported from the GTEx Portal and quantified to summarize evidence for ischemic changes, fibrosis, hypertrophy and infarction.

2.8 Data Availability

GTEx expression data for GRX2 are available at: https://www.gtexportal.org/home/gene/GLRX2. Similar expression data for SIRT3 are

available at: https://www.gtexportal.org/home/gene/SIRT3. GTEx pathological notes are available using the GTEx Histology Image Viewer: https://gtexportal.org/home/histologyPage. The data were obtained from the GTEx Portal on 04/19.

2.9 Statistical Analysis

Data were analyzed using SigmaPlot version 14.0 (Systat software) using one-way ANOVA for comparisons within several groups. Data were transformed when they were not normally distributed, followed by one-way ANOVA with the Holm-Sidak or the Tukey post-hoc test, as indicated. All data are presented as means +/- SEM. Linear correlations of data from the GTEx databank were determined using Pearson correlations.

3.0 Results

3.1 GRX2 and/or SIRT3 expression in cardiac tissue were increased in single knockout mice

SIRT3 and GRX2 knockout was confirmed through the absence of bands in cardiac tissue from the *Sirt3*$^{-/-}$ or the double knockout, *Grx2*$^{-/-}$/*Sirt3*$^{-/-}$ mice. In addition, we found that SIRT3 protein expression was elevated in the *Grx2*$^{-/-}$ heart and GRX2 expression was upregulated in the *Sirt3*$^{-/-}$ heart suggesting that in both single knockouts the upregulation of one system was compensatory for the elimination of the other (Figure 1).

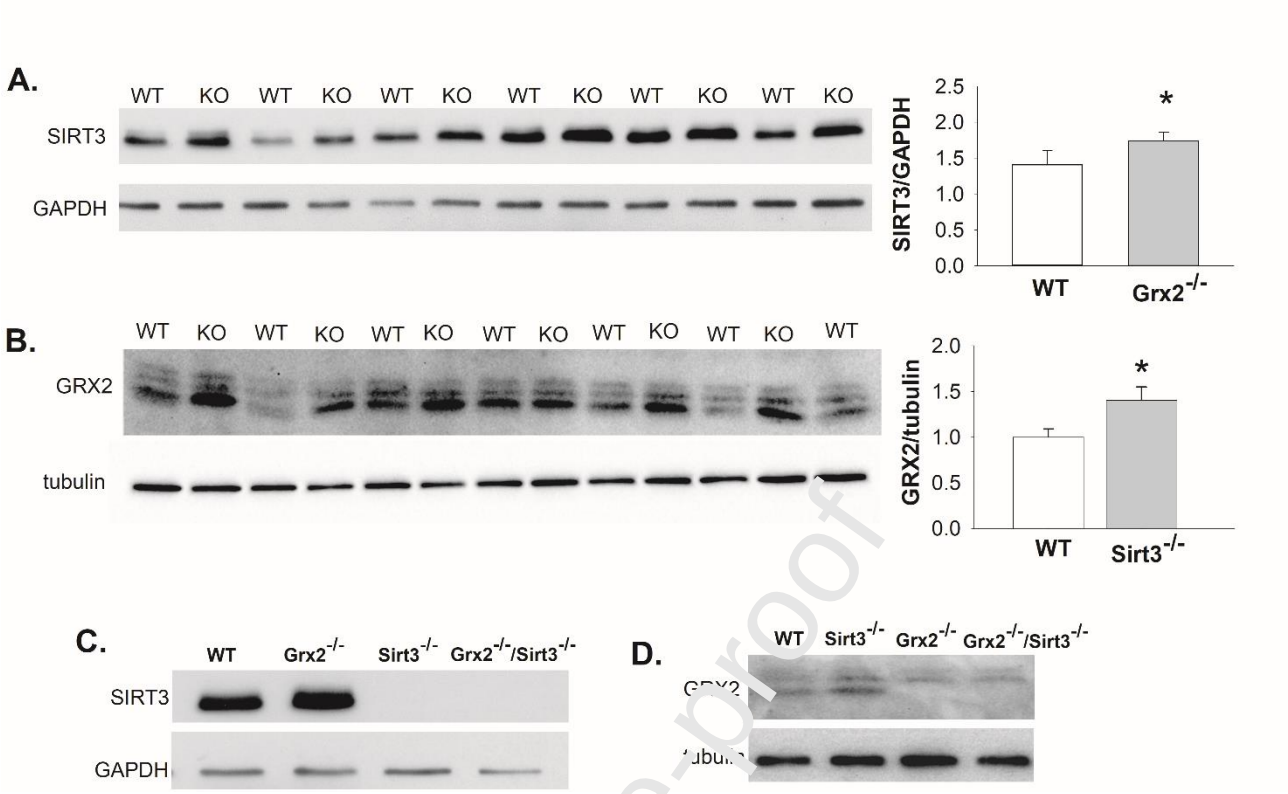

Figure 1. SIRT3 and GRX2 protein expression in cardiac homogenate. A) SIRT3 expression is upregulated in hearts *Grx2*$^{-/-}$ mice and B) GRX2 is upregulated in hearts from *Sirt3*$^{-/-}$ mice. SIRT3 and GRX2 were quantified and normalized to GAPDH and tubulin, respectively. C and D: Representative western blots of pooled samples from wildtype (WT), *Grx2*$^{-/-}$, *Sirt3*$^{-/-}$, and *Grx2*$^{-/-}$/*Sirt3*$^{-/-}$, demonstrating expression of SIRT3 (C), and GRX2 (D) for all groups. N=3-6. Data are normalized to wildtype, and bar graphs represent the mean ± SE. Students' t-tests were used to test for differences between WT and *Sirt3*$^{-/-}$ or *Grx2*$^{-/-}$ (A and B). *p<0.05 vs. WT.

3.2 Increased cardiac hypertrophy in Grx2$^{-/-}$*, Sirt3*$^{-/-}$ *and Grx2*$^{-/-}$*/Sirt3*$^{-/-}$ *mice*

Body weights did not differ between the genotypes at 10-12 weeks of age. However, heart weights were significantly higher in the *Sirt3*$^{-/-}$ mice, compared to wild-type (p=0.011). Cardiac hypertrophy was demonstrated by a modest increase in the heart weight (HW) over body weight (BW) ratios in all of the genotypes, as compared to wildtype (p=0.031, p=0.012 and p=0.041 and for *Grx2*$^{-/-}$, *Sirt3* $^{-/-}$ and for *Grx2*$^{-/-}$*/Sirt3* $^{-/-}$, respectively) (Figure 2A). However, there were no differences in cardiac hypertrophy between the single and double knockout mouse groups.

3.3 Increased cardiac fibrosis in Sirt3$^{-/-}$ and Grx2$^{-/-}$/Sirt3$^{-/-}$ mice

Heart sections from *Sirt3* $^{-/-}$ mice had significantly increased Sirius Red staining, indicative of increased fibrosis (p=0.025, Figure 2B) as compared to wildtype. *Grx2*$^{-/-}$ mice displayed a trend towards increased fibrosis (p=0.07). In *Grx2*$^{-/-}$/*Sirt3* $^{-/-}$ mouse hearts there was significantly increased levels of fibrosis versus wildtype (p=0.029). However, there were no differences in levels of cardiac fibrosis between the single and double knockout mouse groups.

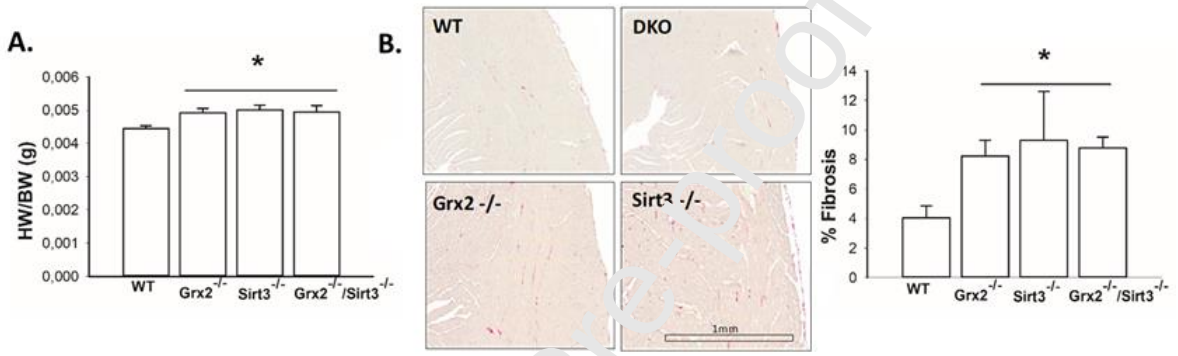

Figure 2. Increased hypertrophy and fibrosis in cardiac tissue from single and double knockout mice. A) Heart weight (HW) normalized to body weight (BW) is higher in all groups as compared to wildtype (WT). B) Sirius red staining is increased in *Grx2*$^{-/-}$/*Sirt3*$^{-/-}$ (top right), *Grx2*$^{-/-}$ (bottom left) and *Sirt3*$^{-/-}$ (bottom right) as compared to wildtype (top left); quantified results are shown in the bar graph. N=9-14. Data are expressed as mean ± SE. One-way ANOVA and Holm-Sidak post hoc test, *p<0.05 vs. WT.

3.4 Increased protein glutathionylation in heart tissue from Grx2$^{-/-}$ and Grx2$^{-/-}$/Sirt3$^{-/-}$ mice

Glutathionylated cardiac protein levels were slightly elevated in both *Grx2*$^{-/-}$ and *Grx2*$^{-/-}$ /*Sirt3* $^{-/-}$ samples, as compared to wildtype (p=0.03 and p=0.04, respectively; Figure 3A). However, levels were not different between the wildtype and *Sirt3*$^{-/-}$ mouse hearts.

3.5 Increased protein acetylation in heart tissue from Sirt3$^{-/-}$ and Grx2$^{-/-}$/Sirt3$^{-/-}$ mice

In line with the well documented deacetylase function of SIRT3, both *Sirt3*$^{-/-}$ and *Grx2*$^{-/-}$ /*Sirt3* $^{-/-}$ samples displayed hyper-acetylation of proteins (p=0.004 and p=0.009 for *Sirt3*$^{-/-}$

and *Grx2*$^{-/-}$/*Sirt3* $^{-/-}$, respectively), as compared to wildtype and *Grx2*$^{-/-}$ mouse hearts (Figure 3B). There were no differences in overall acetylation levels between *Grx2*$^{-/-}$ and wildtype mouse hearts.

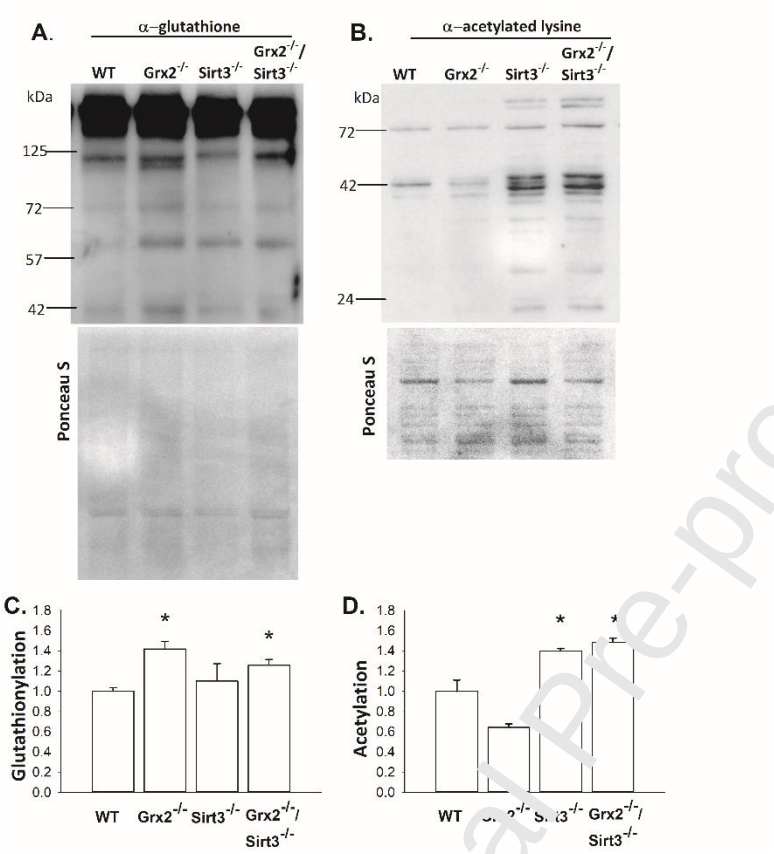

Figure 3. GRX2 and SIRT3 deficiency increases levels of glutathionylation and acetylation in the heart, respectively. A) Global acetylated lysine residues are elevated in hearts from *Sirt3*$^{-/-}$ and *Grx2*$^{-/-}$/*Sirt3*$^{-/-}$ mice and B) Global levels of glutathionylation are increased in cardiac tissue from *Grx2*$^{-/-}$ and *Grx2*$^{-/-}$/*Sirt3*$^{-/-}$ mice. Quantifications of expression of the indicated modification are normalized to wildtype. N=4-8. Data are expressed as mean ± SE. One-way ANOVA and Tukey post hoc test, *p<0.05 vs. WT.

3.6 Impaired mitochondrial respiration in cardiac fibers from Grx2$^{-/-}$*, Sirt3*$^{-/-}$ *and Grx2*$^{-/-}$*/Sirt3*$^{-/-}$ *mice*

In permeabilized cardiac fibers from *Grx2*$^{-/-}$ mice we found lower Complex I-associated proton leak (CI-Leak, Figure 4A), Complex I-associated coupled respiration (CI-OXPHOS, Figure 4B) as well as lower rate of non-phosphorylating respiration following the addition of the F_0F_1-ATPase inhibitor, oligomycin (CI+CII-Leak, Figure 4D) and lower Complex IV-

associated respiration (Figure 4E), as compared to wildtype. Moreover, OXPHOS coupling efficiency (1-(CI-Leak/CI-OXPHOS)) was reduced in cardiac mitochondria from *Grx2*$^{-/-}$ mice (p=0.031, Figure 4F).

In cardiac fibers from *Sirt3*$^{-/-}$ mice, CI-Leak was lower as compared to wildtype hearts (p=0.011, Figure 4A). There was also a trend towards lower CI-OXPHOS in *Sirt3*$^{-/-}$ as compared to wild-type (p=0.084, Figure 4B); however, this did not reach significance. Despite lower CI-Leak respiration in the *Sirt3*$^{-/-}$, the OXPHOS coupling efficiency remained unchanged. Surprisingly, we did not observe exacerbated effects on mitochondrial respiration rates due to the double knockout. In cardiac fibers from *Grx2*$^{-/-}$/*Sirt3*$^{-/-}$ mice, CI-Leak respiration was not significantly lower, while this was the case in both *Grx2*$^{-/-}$ and *Sirt3*$^{-/-}$ hearts. CI-OXPHOS was lower in the *Grx2*$^{-/-}$/*Sirt3*$^{-/-}$ cardiac fibers as compared to wildtype (Figure 4B), and accordingly OXPHOS coupling efficiency was also reduced in these hearts (p=0.031, Figure 4F). Maximal OXPHOS capacity (CI&CII-associated coupled respiration) was not different between the genotypes although there was a trend that this was lower in all groups as compared to wild type (p=0.096 between groups, Figure 4C).

Importantly, there were no differences between groups in tissue mitochondrial content, as measured by citrate synthase activity (Figure 4G). As well, neither the single nor double knockout of GRX2 and SIRT3 significantly altered the protein expression of OXPHOS complex subunits as assessed by western blotting analysis (Figure 4H).

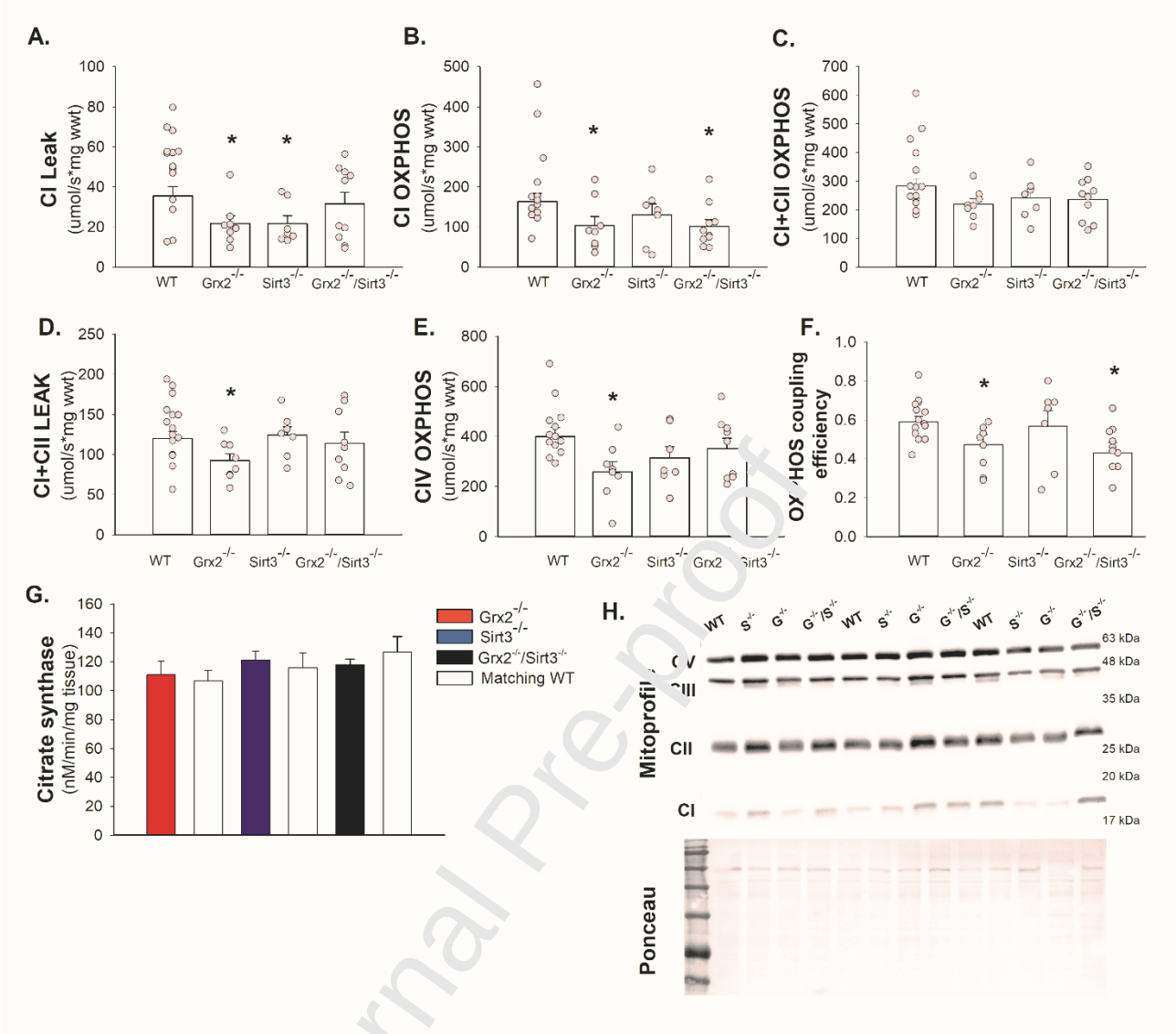

Figure 4. Evaluation of mitochondrial respiration and respiratory complexes. A-E) Mitochondrial respiration measured in permeabilized cardiac fibers and F) OXPHOS coupling efficiency calculated from 1-(CI-Leak/CI-OXPHOS). G) Quantification of citrate synthase activity. N= 8-14. H) OXPHOS protein levels were determined and normalized to Ponceau stains. N=5-7. Bar graphs represent the mean ± SE, and individual experiments are represented in the scatter plots. One-way ANOVA and Holm-Sidak post hoc tests were used for statistical analysis, and data were transformed in B and C to achieve normal distributions, *p<0.05 vs. WT.

3.7 Differences in H_2O_2 emission in cardiac fibers in Sirt3$^{-/-}$ without marked changes in glutathione redox

Oxidative stress was characterized by the ratio of H_2O_2 production rate/O_2 consumption in cardiac fibers. We found H_2O_2/O_2 flux to be higher in the *Sirt3*$^{-/-}$ hearts during bioenergetic conditions of: CI-Leak, CI&CII-associated coupled (CI&CII maximal capacity) and CI&CII-Leak (oligomycin-induced) as compared to wildtype (p=0.009, p=0.011 and p=0.005, respectively; Figure 5). We did not observe any changes in the *Grx2*$^{-/-}$ cardiac fibers, nor did we find a significantly higher H_2O_2/O_2 flux cardiac fibers from *Grx2*$^{-/-}$/*Sirt3*$^{-/-}$, where H_2O_2 emission was unaltered as compared to wildtype for all respiration states. Thus, the absence of SIRT3 enhanced H_2O_2 emission in cardiac fibers, however, in the *Grx2*$^{-/-}$/*Sirt3* $^{-/-}$ heart tissues, H_2O_2 emissions were comparable to wildtype concentrations. As GRX2 activity alters glutathione redox environment, we also measured glutathione levels (*i.e.*, GSH, GSSG and GSH:GSSG) in cardiac tissue. Although the GSH:GSSG ratio in the *Grx2*$^{-/-}$ heart tended to be lower, there were no significant differences as compared to wildtype (p=0.157, Figure 5E), and unaltered in hearts from *Grx2*$^{-/-}$/*Sirt3*$^{-/-}$ mice. Furthermore, GSH and GSSG levels within the single and double knockout groups were not significantly different (Figure 5E). H_2O_2 levels are, under normal conditions, quenched by antioxidant systems such as the glutathione system which utilizes GPX. Accordingly, GPX4 was upregulated in cardiac tissue from Sirt3$^{-/-}$ however remained unchanged in *Grx2*$^{-/-}$ and *Grx2*$^{-/-}$/*Sirt3*$^{-/-}$ as compared to wildtype (Figure 5F).

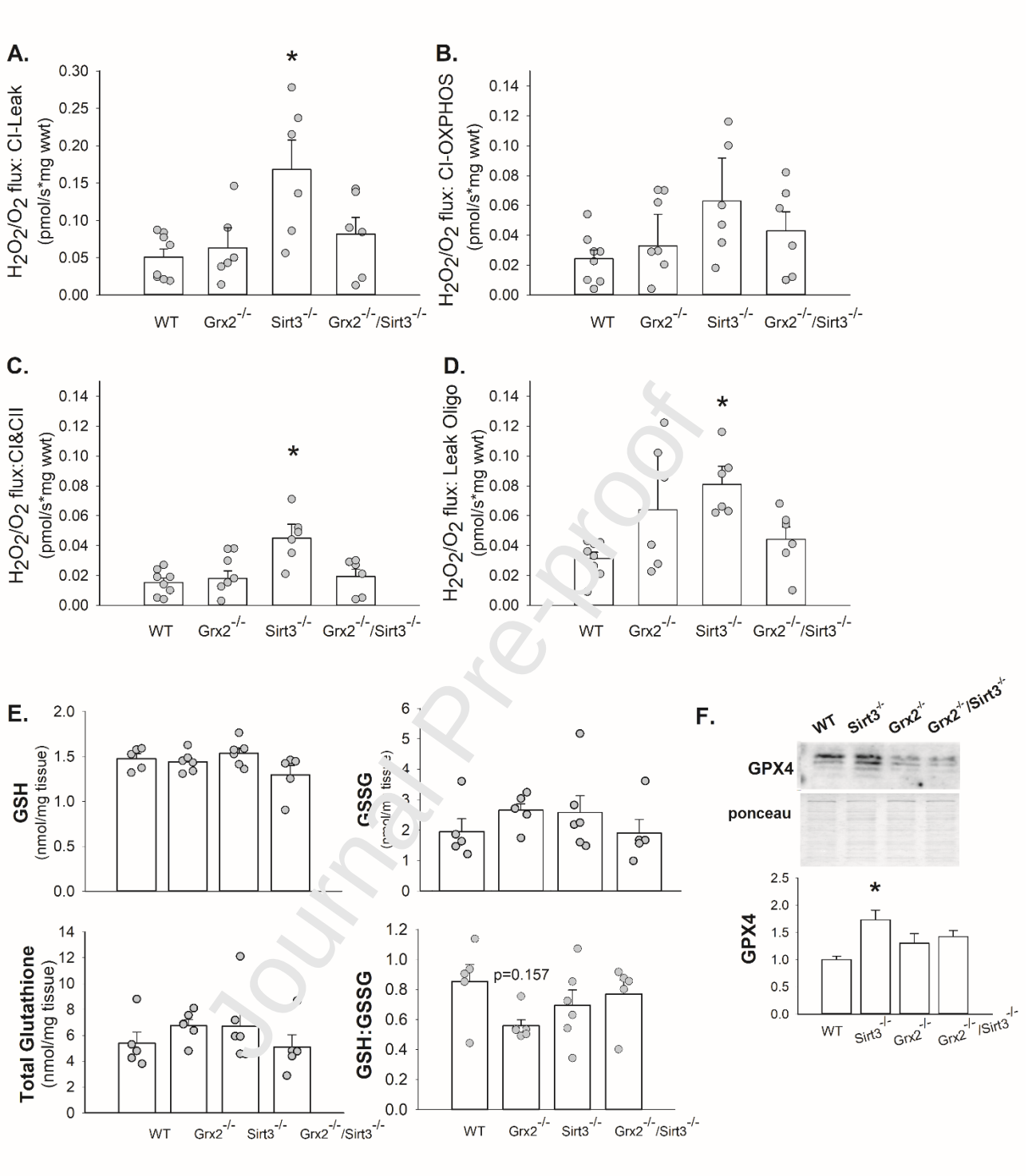

Figure 5. Oxidative stress-related measurements in myocardial tissue. H_2O_2 production/O_2 consumption in permeabilized fibers was increased in *Sirt3*$^{-/-}$ hearts. A-D) H_2O_2 was determined by Amplex UltraRed, in the presence of superoxide dismutase and horseradish peroxidase, during different states of mitochondrial respiration. N=6-8. E) Redox changes were assessed by GSH and GSSG levels in all groups, their sum (total glutathione) and by the GSH:GSSG ratio. F) GPX4 protein was elevated in *Sirt3*$^{-/-}$ mouse hearts, as quantified

by western blot. N=5-7. Bar graphs represent the mean ± SE, and individual experimental determinations are represented in the scatter plots. One-way ANOVA and Holm-Sidak post hoc test were used for statistical analysis, *p<0.05 vs. WT.

3.7 Human left ventricle SIRT3 expression is inversely correlated with cardiac pathologies

To evaluate human left ventricle levels of SIRT3 expression and a role for SIRT3 in human heart disease, we examined cardiac tissue samples downloaded from the GTEx consortium, corresponding to 228 individual samples (GTEx, 2018). We then sorted GTEx left ventricle samples into those that expressed the lowest and highest SIRT3 transcript levels (N=50 per group). The data sets also included hematoxylin and eosin (H&E) stained histological sections and corresponding pathologists' notes, that were used to compare histopathological phenotypes from the 50 highest and the 50 lowest SIRT3 expression left ventricle samples. In the low SIRT3 expressors, there was evidence of moderate to extensive interstitial fibrosis, greater incidence of hypertrophic myofibers, increased ischemic changes and evidence of infarcted tissue, as compared to samples from high SIRT3 expressors. These findings suggest an inverse correlation between SIRT3 expression and the incidence of pathological changes in the heart, associated with ischemia, moderate to extensive fibrosis, left ventricle hypertrophy and infarction (Figure 6B).

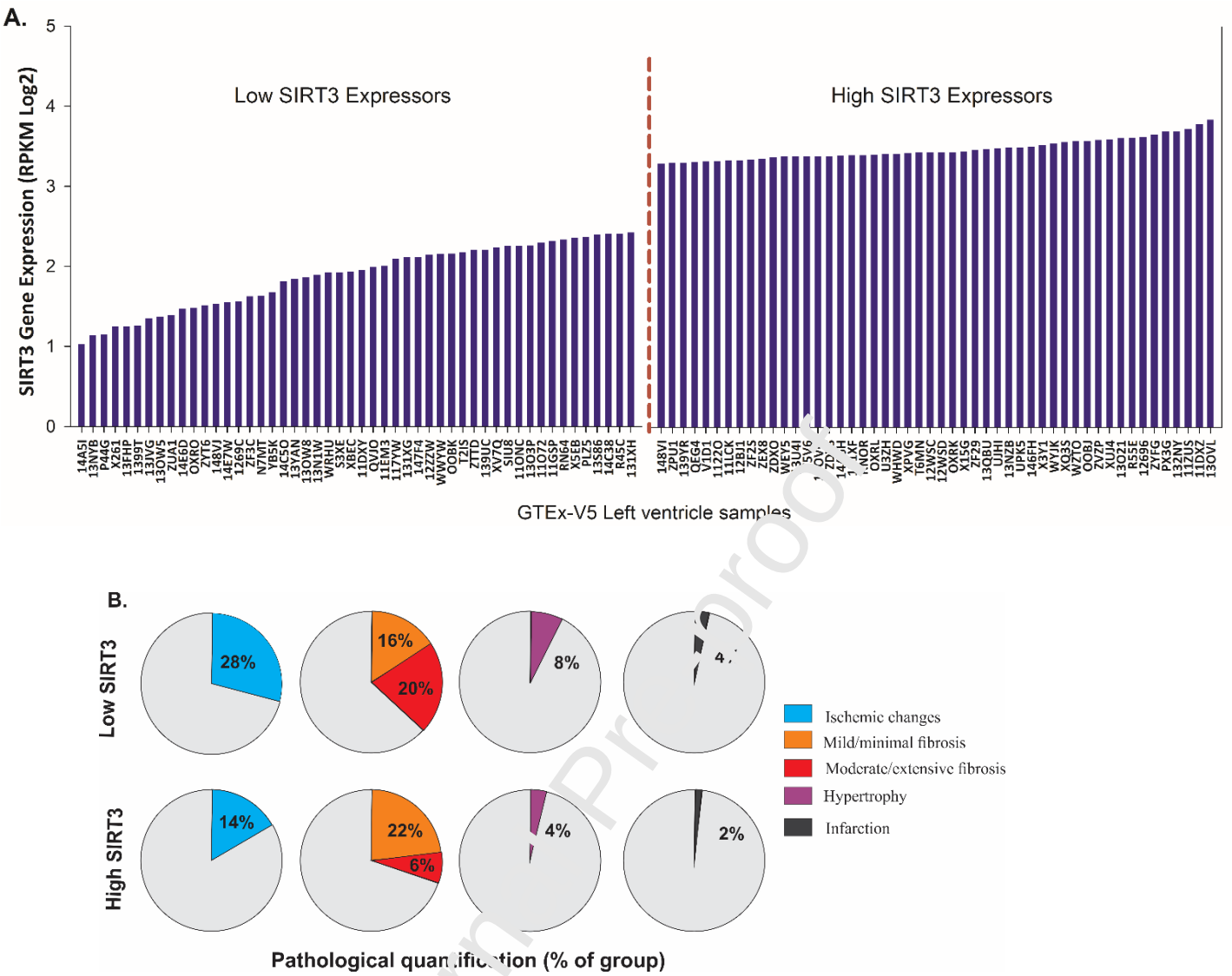

Figure 6. Low Sirtuin 3 (SIRT3) expression in the left ventricle correlates with increased ischemic changes, fibrosis, hypertrophy and infarct in human data downloaded from GTEx. A) SIRT3 transcript expression levels in left ventricle samples. RPKM refers to Reads Per Kilobase of transcript per Million mapped reads and is expressed in log2 values. After sorting we selected data sets from the lowest and the highest SIRT3 expressors (N=50 per group). B) Evidence for pathological changes associated with ischemia, fibrosis, hypertrophy and infarction in left ventricle heart samples from the low and high SIRT3 groups, summarized from notes corresponding to H&E histological sections downloaded from GTEx.

3.8 Grx2 and SIRT3 expression levels are positively correlated in human left ventricle

To evaluate the potential relationship between SIRT3 and GRX2 in the human heart, transcript expression levels were analyzed (Figure 7A). Here, we found a significant positive correlation of +0.49 for SIRT3 and GRX2 (Figure 7B). Interestingly, both SIRT3 and GRX2 were also found to be positively correlated with both SOD1 and SOD2 (Figure 8). However, we did not observe significantly altered levels of either SOD1 or SOD2 between the single and the double knockouts, or as compared to wildtype (Figure 8E and 8F).

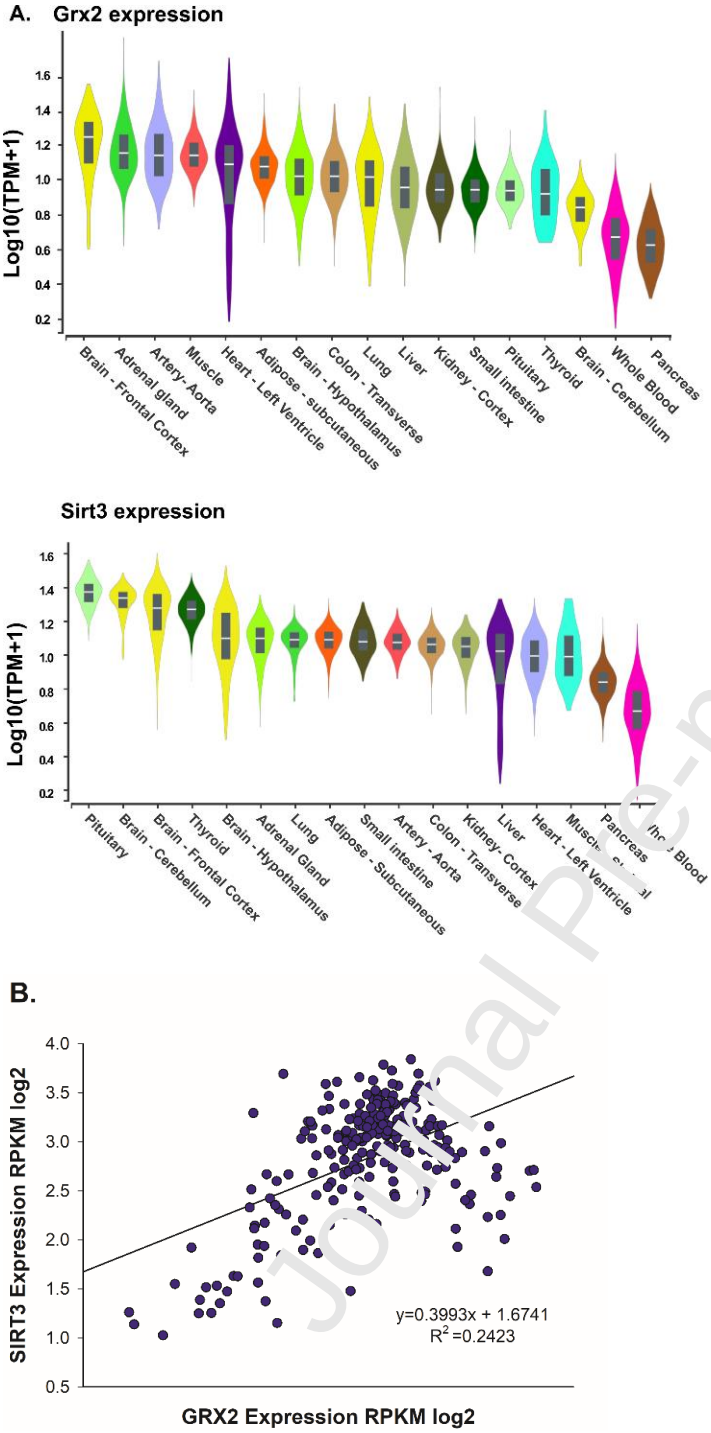

Figure 7. SIRT3 and GRX2 transcript levels in various tissues and their positive correlation in human left ventricle samples, downloaded from GTEx. A) SIRT3 and GRX2 transcript expression levels for various tissues obtained from the human GTEx database. Values are presented as transcripts per million (TPM), with box plots denoting median, 25th and 75th percentile values. B) Correlation of SIRT3 and GRX2 human left ventricle expression levels, presented in RPKM (Reads Per Kilobase of transcript per Million mapped reads) log2 values. Pearson correlation coefficient: 0.49 (p= 2.1 E-16).

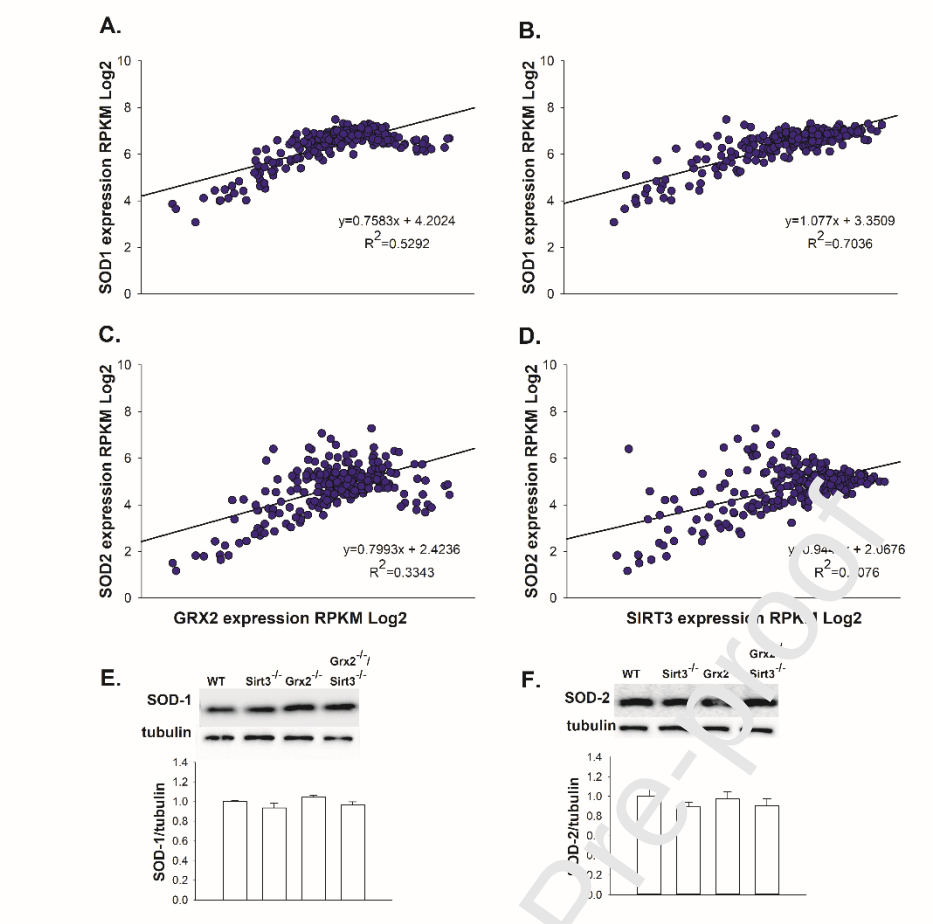

Figure 8. SOD1 and SOD2 expression levels in human and mouse cardiac tissues. A-D) SIRT3 and GRX2 are each positively correlated with SOD1 and SOD2 transcript levels in the human left ventricle. Data from the GeneNetwork program, and presented as RPKM log2 values. Pearson correlation coefficients: A) 0.73 (p=8.5 E-42); B) 0.84 (p=2.3 E-66); C) 0.58 (p= 2.4 E-23); and D) 0.55 (p= 3.1 E-21). E) Representative western blots and quantification of SOD1 and F) SOD2 from single and double knockout mouse hearts. N=5-6. Data are normalized to wildtype, and bar graphs represent the mean ± SE. One-way ANOVA and Holm-Sidak post hoc tests were used for statistical analysis, *p<0.05 vs. WT.

4.0 Discussion

Altered redox signaling and oxidative stress are heavily implicated in the progression of heart failure. Both GRX2 and SIRT3 have been associated with protection from oxidative damage in the myocardium. Based on preliminary findings that SIRT3 increased in response to Grx2 knockout, and GRX2 increased in response to Sirt3 knockout, we hypothesized that these were compensatory mechanisms to counteract the detrimental effects when either GRX2 or SIRT3 was deficient. Through analysis of human expression data from the GTEx database and associated tissue bank, our analyses show a positive correlation between GRX2 and SIRT3 expression levels in the left ventricle, and confirm that dysregulated redox systems are important in the failing heart. In the present study, we have demonstrated changes in myocardial fibrosis and hypertrophy as well as a lower mitochondrial capacity in cardiac tissue from the *Grx2*$^{-/-}$ and the *Sirt3*$^{-/-}$ mouse, however this was only associated with elevated H_2O_2 emission in the *Sirt3*$^{-/-}$ mice. Although, similar pathological changes were also observed in the *Grx2*$^{-/-}$/*Sirt3* $^{-/-}$ mouse hearts, there were no apparent additive effects of the double knockout.

SIRT3 has been shown to have a role in cellular detoxification through deacetylation of SOD2 [55], an important enzyme in the mitochondrial antioxidant systems. In the *Sirt3*$^{-/-}$ mouse heart, lower SOD2 and antioxidant capacity, in addition to impaired CI-OXPHOS function, was associated with higher levels of oxidative stress [46]. This suggests a role for SIRT3 in handling acute cardiac redox stress, *e.g.,* by ischemia, where diminished SIRT3 resulted in increased ischemic injury. Consistent with this potential role, the elevation of SIRT3 has been demonstrated both in mitochondria and in the nucleus following stress of cardiomyocytes, and likewise the overexpression of SIRT3 protects myocytes from genotoxic and oxidative stress-mediated cell death [54]. Thus, it is possible that consequences of SIRT3 deletion become more apparent during conditions of additional myocardial stress such as trans-aortic banding (TAC) or aging. Despite lower mitochondrial respiration, Koentges *et al* did not observe signs of altered acetylation levels of SOD2 in 8-week old *Sirt3*$^{-/-}$ mouse hearts [27]. Moreover, they did not find any improvements in cardiac dysfunction following targeted treatment of oxidative stress and have suggested that cytosolic ROS was not the cause of cardiac dysfunction in the SIRT3 KO mouse. In the present study, “real-time” H_2O_2 emission (in parallel with respiration) was consistently higher for all respiration states in the *Sirt3*$^{-/-}$ cardiac fibers as compared to

wild-type. The elevations in H_2O_2 emissions were also associated with changes in expression of GPX4. In contrast, there were no changes in SOD1, SOD2 or in glutathione redox. As persistent oxidative stress is considered important in the progression of hypertrophy [38] and the reversal of oxidative stress through SIRT3 overexpression can prevent pathological remodeling [17, 44, 53], our findings of elevated H_2O_2 emission in *Sirt3*$^{-/-}$ cardiac fibers, may be causative for increased hypertrophy although the mechanisms remain unclear. Accordingly, cardiac hypertrophy has been shown in male *Sirt3*$^{-/-}$ at 10-12 weeks (present study), and at 24 weeks, but not at 8 weeks [27].

In accordance with previous studies, we have confirmed that the full deletion of GRX2 also results in the development of hypertrophy [32], in addition to cardiac ultrastructure changes including cardiac fibrosis [24, 33, 34]. H_2O_2 emission was not elevated in cardiac fibers from *Grx2*$^{-/-}$ mice [28] although GRX2 can alter glutathione redox [24, 34]. In contrast, higher GRX2-mediated superoxide and H_2O_2 release from CI and CIII has been reported in cardiac mitochondria in the *Grx2*$^{-/-}$ mouse heart compared to wild-type, especially during succinate-driven respiration [10]. The lack of increase in H_2O_2 release during CI or CI+CII-driven respiration (i.e., including succinate as substrate) in the present study may be due to differences in the use of mitochondrial versus permeabilized cardiac fiber preparations. As GRX2 and SIRT3 were shown to play a role in the pathological remodeling of the heart, it was surprising that the absence of both GRX2 and SIRT3 did not worsen hypertrophy or fibrosis, nor did the double knockout enhance H_2O_2 emission from mitochondria. The upregulation of SOD1 and SOD2, as a compensatory mechanism for GRX2 and SIRT3 absence, was not observed here. Although glutathione redox was not markedly disturbed in the double knockout we were unable to determine an underlying mechanism that might indicate additive effects of the double knockout.

Heart failure with hypertrophy has been associated with energetic deficit [42] and metabolic inflexibility [26] has been linked to altered capacity of the mitochondria to meet energetic needs of the heart [8]. Accordingly, previous studies have demonstrated a severely impaired metabolic flexibility as well as mitochondrial OXPHOS in cardiomyocytes isolated from *Grx2*$^{-/-}$ mice, suggesting that glutathionylation is critical in modulating mitochondrial ATP output in cardiac muscle, and disruption of this process leads to a pathological outcome [24, 34]. On the other hand, the deacetylation of CI in cardiac mitochondria is regulated by SIRT3, and its deletion has been shown to result in impaired CI function [25, 46, 48]. Based on this, we hypothesized that deletion of SIRT3

paired with GRX2 knockout, would exacerbate impaired mitochondrial OXPHOS in the *Grx2*$^{-/-}$/*Sirt3*$^{-/-}$. Although we found mitochondrial energetics to be impaired, the effects of the double knockout were not additive. In the present study, we evaluated OXPHOS-coupling efficiency, to indicate whether mitochondrial dysfunction was related to ADP-driven or leak-driven respiration [9]. We found that lower OXPHOS-coupling efficiency in the *Grx2*$^{-/-}$ and the *Grx2*$^{-/-}$/*Sirt3*$^{-/-}$ mouse hearts are both linked to lower CI-OXPHOS. In the *Sirt3*$^{-/-}$, although CI-Leak was lower compared to wild-type, this did not significantly alter OXPHOS-coupling efficiency. Additionally, in *Grx2*$^{-/-}$ cardiac fibers, there was lower oligomycin-induced leak respiration. Given that OXPHOS and uncoupled respiration were significantly decreased in *Grx2*$^{-/-}$ cardiac fibers, this may be indicative of decreased activity of a respiratory complex or complexes rather than decreased ATP synthase activity [34]. Mitochondrial respiratory chain deficiencies have been documented in a wide range of human disease. Recently, chronic hypoxic exposure has been reported to activate endogenous hypoxic responses, thus preventing the onset of pathological defects within the CI respiratory complex [22]. These findings suggest that defective oxygen signaling or toxicity may be at the root of various types of mitochondrial disease. Similarly, in the heart, partial CI-inhibition can attenuate oxidative stress without impairing ATP production, and this has been reported to be cardioprotective during conditions such as ischemia-reperfusion [12, 37]. It is possible that the lack of additive effects observed in the double knockout model in the present study may be due to the combined effect of repressed respiration and redox thereby minimizing accumulation of toxic oxygen intermediates. Thus, it is also possible that in the present study, repressed CI-OXPHOS in the absence of both SIRT3 and GRX2 is not associated with a worsened phenotype in the double knockout.

The assembly of mitochondrial respiratory complexes into supramolecular structures known as respiratory supercomplexes and/or into more complex levels of higher order respiratory strings, play a role in the regulation of OXPHOS as well as in ROS production [1, 60]. Although depressed OXPHOS was not associated with altered levels of OXPHOS proteins, this does not exclude altered association of the individual complexes into respirosomes or the impaired stability of the individual complexes within the supercomplexes.

Finally, our findings show through examining GTEx data that in adult humans there is a significant positive correlation between GRX2 and SIRT3 expression levels in the left ventricle. Previously, an inverse correlation between GRX2 expression levels and adverse cardiac pathology was established, whereby individuals characterized as low GRX2 expressors were found to have increased incidence of moderate fibrosis, hypertrophy and infarct [24]. Here, we present a similar trend with regard to cardiac SIRT3 expression levels wherein low SIRT3 expressors displayed increased incidence of ischemic changes, moderate to extensive fibrosis, hypertrophy, and infarct. Although some experimental mouse studies [25, 44] have shown both GRX2 and SIRT3 to be associated with lowered levels of the superoxide dismutases (SOD1 and SOD2), we did not observe changes in SOD1 or SOD2 in the deletion models studied here. In heart failure, this would indicate a strongly diminished capacity for ROS detoxification by major antioxidant systems that are known to counteract cardiac stress.

In the absence of SOD1/2 upregulation, the question remains – what other mechanisms are available within the myocardium to counter oxidative damage? One possible explanation lies in the complex variety of protective mechanisms found in crucial organs, such as the heart. Low levels of small ubiquitin-like modifier mediated modification (SUMOylation) has been shown to contribute to cardiac dysfunction and disease progression (39). In addition, phosphorylation [13], succinylation [65], and O-GlcNAcylation [31] are PTMs that may also contribute to pathological hypertrophy [62]; however these were not assessed in the present study. Finally as noted above, it is also possible that re-organization of the respiratory supercomplexes may compensate for enhanced oxidative stress, as ROS has been shown to modulate supercomplex assembly [4].

In summary, although both SIRT3 and GRX2 are implicated in protection from oxidative damage, and are downregulated in patients with cardiac disease, in the *Sirt3*$^{-/-}$*/Grx2*$^{-/-}$ mouse, we did not observe exacerbated effects on structural remodelling or mitochondrial function versus the individual knockouts. The findings from the GTEx analyses would suggest that in humans with heart disease, both SIRT3 and GRX2 expression levels would be lowered. Perhaps then the *Sirt3*$^{-/-}$*/Grx2*$^{-/-}$ is a more representative mouse model for heart failure. Taken together, redox signaling is required for multiple cellular processes in the heart, and dysregulation within redox signaling contributes to myocardial remodelling and impaired mitochondrial function. Cross-talk between systems involved in PTMs such

as glutathionylation and acetylation, might benefit the heart under conditions of stress, and strengthen overall antioxidant capacity.

Author Contributions:

MEH conceived the idea for the project. NTB, BM, and CP performed all experiments to assess mitochondrial function, and NTB analyzed the data. BM performed immunoblotting. CP and GP performed immunoblotting, glutathione analyses and respiratory complex activity. BM acquired the human data from GTEx consortium, and the data was analyzed by BM and KM. NTB and MEH wrote the paper and all authors reviewed and approved it.

Acknowledgements:

Authors are grateful for the help of the members of the University of Ottawa Pathology Laboratory for their histological work.

Funding:

This research was supported by the Canadian Institutes of Health Research (FDN 143278 to MEH). N.T Boardman was supported by a Norwegian Health Association post-doctoral scholarship.

References

1. Acin-Perez R, Enriquez JA (2014) The function of the respiratory supercomplexes: the plasticity model. Biochim Biophys Acta 1837:444-450. doi:10.1016/j.bbabio.2013.12.009
2. Ahn BH, Kim HS, Song S, Lee IH, Liu J, Vassilopoulos A, Deng CX, Finkel T (2008) A role for the mitochondrial deacetylase Sirt3 in regulating energy homeostasis. Proc Natl Acad Sci U S A 105:14447-14452. doi:10.1073/pnas.0803790105
3. Alrob OA, Sankaralingam S, Ma C, Wagg CS, Fillmore N, Jaswal JS, Sack MN, Lehner R, Gupta MP, Michelakis ED, Padwal RS, Johnstone DE, Sharma AM, Lopaschuk GD (2014) Obesity-induced lysine acetylation increases cardiac fatty acid oxidation and impairs insulin signalling. Cardiovasc Res 103:485-497. doi:10.1093/cvr/cvu156
4. Anwar MR, Saldana-Caboverde A, Garcia S, Diaz F (2018) The Organization of Mitochondrial Supercomplexes is Modulated by Oxidative Stress In Vivo in Mouse Models of Mitochondrial Encephalopathy. Int J Mol Sci 19. doi:10.3390/ijms19061582
5. Balaban RS, Nemoto S, Finkel T (2005) Mitochondria, oxidants, and aging. Cell 120:483-495. doi:10.1016/j.cell.2005.02.001
6. Beer SM, Taylor ER, Brown SE, Dahm CC, Costa NJ, Runswick MJ, Murphy MP (2004) Glutaredoxin 2 catalyzes the reversible oxidation and glutathionylation of mitochondrial membrane thiol proteins: implications for mitochondrial redox regulation and antioxidant DEFENSE. J Biol Chem 279:47939-47951. doi:10.1074/jbc.M408011200
7. Berndt C, Lillig CH, Holmgren A (2007) Thiol-based mechanisms of the thioredoxin and glutaredoxin systems: implications for diseases in the cardiovascular system. Am J Physiol Heart Circ Physiol 292:H1227-1236. doi:10.1152/ajpheart.01152.2006
8. Bertero E, Maack C (2018) Metabolic remodelling in heart failure. Nat Rev Cardiol 15:457-470. doi:10.1038/s41569-018-0044-6
9. Brand MD, Nicholls DG (2011) Assessing mitochondrial dysfunction in cells. Biochem J 435:297-312. doi:10.1042/BJ20110162
10. Chalker J, Gardiner D, Kuksal N, Mailloux RJ (2018) Characterization of the impact of glutaredoxin-2 (GRX2) deficiency on superoxide/hydrogen peroxide release from cardiac and liver mitochondria. Redox Biol 15:216-227. doi:10.1016/j.redox.2017.12.006
11. Chen M, Fu H, Zhang J, Huang H, Zhong P (2019) CIRP downregulation renders cardiac cells prone to apoptosis in heart failure. Biochem Biophys Res Commun 517:545-550. doi:10.1016/j.bbrc.2019.05.012
12. Chouchani ET, Methner C, Nadtochiy SM, Logan A, Pell VR, Ding S, James AM, Cocheme HM, Reinhold J, Lilley KS, Partridge L, Fearnley IM, Robinson AJ, Hartley RC, Smith RA, Krieg T, Brookes PS, Murphy MP (2013) Cardioprotection by S-nitrosation of a cysteine switch on mitochondrial complex I. Nat Med 19:753-759. doi:10.1038/nm.3212
13. Deng N, Zhang J, Zong C, Wang Y, Lu H, Yang P, Wang W, Young GW, Wang Y, Korge P, Lotz C, Doran P, Liem DA, Apweiler R, Weiss JN, Duan H, Ping P (2011) Phosphoproteome analysis reveals regulatory sites in major pathways of cardiac mitochondria. Mol Cell Proteomics 10:M110 000117. doi:10.1074/mcp.M110.000117
14. Enoksson M, Fernandes AP, Prast S, Lillig CH, Holmgren A, Orrenius S (2005) Overexpression of glutaredoxin 2 attenuates apoptosis by preventing cytochrome c release. Biochem Biophys Res Commun 327:774-779. doi:10.1016/j.bbrc.2004.12.067
15. Fukushima A, Lopaschuk GD (2016) Acetylation control of cardiac fatty acid beta-oxidation and energy metabolism in obesity, diabetes, and heart failure. Biochim Biophys Acta 1862:2211-2220. doi:10.1016/j.bbadis.2016.07.020
16. Gao XH, Qanungo S, Pai HV, Starke DW, Steller KM, Fujioka H, Lesnefsky EJ, Kerner J, Rosca MG, Hoppel CL, Mieyal JJ (2013) Aging-dependent changes in rat heart mitochondrial glutaredoxins--Implications for redox regulation. Redox Biol 1:586-598. doi:10.1016/j.redox.2013.10.010

17. Graham D, Huynh NN, Hamilton CA, Beattie E, Smith RA, Cocheme HM, Murphy MP, Dominiczak AF (2009) Mitochondria-targeted antioxidant MitoQ10 improves endothelial function and attenuates cardiac hypertrophy. Hypertension 54:322-328. doi:10.1161/HYPERTENSIONAHA.109.130351
18. Hanschmann EM, Godoy JR, Berndt C, Hudemann C, Lillig CH (2013) Thioredoxins, glutaredoxins, and peroxiredoxins--molecular mechanisms and health significance: from cofactors to antioxidants to redox signaling. Antioxid Redox Signal 19:1539-1605. doi:10.1089/ars.2012.4599
19. Hirschey MD, Shimazu T, Goetzman E, Jing E, Schwer B, Lombard DB, Grueter CA, Harris C, Biddinger S, Ilkayeva OR, Stevens RD, Li Y, Saha AK, Ruderman NB, Bain JR, Newgard CB, Farese RV, Jr., Alt FW, Kahn CR, Verdin E (2010) SIRT3 regulates mitochondrial fatty-acid oxidation by reversible enzyme deacetylation. Nature 464:121-125. doi:10.1038/nature08778
20. Hirschey MD, Shimazu T, Huang JY, Verdin E (2009) Acetylation of mitochondrial proteins. Methods Enzymol 457:137-147. doi:10.1016/S0076-6879(09)05008-3
21. Hofer A, Wenz T (2014) Post-translational modification of mitochondria as a novel mode of regulation. Exp Gerontol 56:202-220. doi:10.1016/j.exger.2014.03.006
22. Jain IH, Zazzeron L, Goli R, Alexa K, Schatzman-Bone S, Dhillon H, Goldberger O, Peng J, Shalem O, Sanjana NE, Zhang F, Goessling W, Zapol WM, Mootha VK (2016) Hypoxia as a therapy for mitochondrial disease. Science 352:54-61. doi:10.1126/science.aad9642
23. Jang S, Javadov S (2018) Elucidating the contribution of ETC complexes I and II to the respirasome formation in cardiac mitochondria. Sci Rep 8:17732. doi:10.1038/s41598-018-36040-9
24. Kanaan GN, Ichim B, Gharibeh L, Maharsy W, Patten DA, Xuan JY, Reunov A, Marshall P, Veinot J, Menzies K, Nemer M, Harper ME (2018) Glutaredoxin 2 controls cardiac mitochondrial dynamics and energetics in mice, and protects against human cardiac pathologies. Redox Biol 14:509-521. doi:10.1016/j.redox.2017.10.019
25. Karamanlidis G, Lee CF, Garcia-Menendez L, Kolwicz SC, Jr., Suthammarak W, Gong G, Sedensky MM, Morgan PG, Wang W, Tian R (2013) Mitochondrial complex I deficiency increases protein acetylation and accelerates heart failure. Cell Metab 18:239-250. doi:10.1016/j.cmet.2013.07.002
26. Karwi QG, Uddin GM, Ho KL, Lopaschuk GD (2018) Loss of Metabolic Flexibility in the Failing Heart. Front Cardiovasc Med 5:68. doi:10.3389/fcvm.2018.00068
27. Koentges C, Pfeil K, Schnick T, Wiese S, Dahlbock R, Cimolai MC, Meyer-Steenbuck M, Cenkerova K, Hoffmann MM, Jaeger C, Odening KE, Kammerer B, Hein L, Bode C, Bugger H (2015) SIRT3 deficiency impairs mitochondrial and contractile function in the heart. Basic Res Cardiol 110:36. doi:10.1007/s00395-015-0493-6
28. Lillig CH, Lonn ME, Enoksson M, Fernandes AP, Holmgren A (2004) Short interfering RNA-mediated silencing of glutaredoxin 2 increases the sensitivity of HeLa cells toward doxorubicin and phenylarsine oxide. Proc Natl Acad Sci U S A 101:13227-13232. doi:10.1073/pnas.0401896101
29. Lonn ME, Hudemann C, Berndt C, Cherkasov V, Capani F, Holmgren A, Lillig CH (2008) Expression pattern of human glutaredoxin 2 isoforms: identification and characterization of two testis/cancer cell-specific isoforms. Antioxid Redox Signal 10:547-557. doi:10.1089/ars.2007.1821
30. Lopaschuk GD, Ussher JR, Folmes CD, Jaswal JS, Stanley WC (2010) Myocardial fatty acid metabolism in health and disease. Physiol Rev. 90:207-258. doi:doi:10.1152/physrev.00015.2009
31. Ma J, Liu T, Wei AC, Banerjee P, O'Rourke B, Hart GW (2015) O-GlcNAcomic Profiling Identifies Widespread O-Linked beta-N-Acetylglucosamine Modification (O-GlcNAcylation) in Oxidative Phosphorylation System Regulating Cardiac Mitochondrial Function. J Biol Chem 290:29141-29153. doi:10.1074/jbc.M115.691741
32. Mailloux RJ, Willmore WG (2014) S-glutathionylation reactions in mitochondrial function and disease. Front Cell Dev Biol 2:68. doi:10.3389/fcell.2014.00068
33. Mailloux RJ, Xuan JY, Beauchamp B, Jui L, Lou M, Harper ME (2013) Glutaredoxin-2 is required to control proton leak through uncoupling protein-3. J Biol Chem 288:8365-8379. doi:10.1074/jbc.M112.442905
34. Mailloux RJ, Xuan JY, McBride S, Maharsy W, Thorn S, Holterman CE, Kennedy CR, Rippstein P, deKemp R, da Silva J, Nemer M, Lou M, Harper ME (2014) Glutaredoxin-2 is required to control

oxidative phosphorylation in cardiac muscle by mediating deglutathionylation reactions. J Biol Chem 289:14812-14828. doi:10.1074/jbc.M114.550574
35. Makrecka-Kuka M, Krumschnabel G, Gnaiger E (2015) High-Resolution Respirometry for Simultaneous Measurement of Oxygen and Hydrogen Peroxide Fluxes in Permeabilized Cells, Tissue Homogenate and Isolated Mitochondria. Biomolecules 5:1319-1338. doi:10.3390/biom5031319
36. Mieyal JJ, Gallogly MM, Qanungo S, Sabens EA, Shelton MD (2008) Molecular mechanisms and clinical implications of reversible protein S-glutathionylation. Antioxid Redox Signal 10:1941-1988. doi:10.1089/ars.2008.2089
37. Mohsin AA, Chen Q, Quan N, Rousselle T, Maceyka MW, Samidurai A, Thompson J, Hu Y, Li J, Lesnefsky EJ (2019) Mitochondrial Complex I Inhibition by Metformin Limits Reperfusion Injury. J Pharmacol Exp Ther 369:282-290. doi:10.1124/jpet.118.254300
38. Morin D, Long R, Panel M, Laure L, Taranu A, Gueguen C, Pons S, Leoni V, Caccia C, Vatner SF, Vatner DE, Qiu H, Depre C, Berdeaux A, Ghaleh B (2019) Hsp22 overexpression induces myocardial hypertrophy, senescence and reduced life span through enhanced oxidative stress. Free Radic Biol Med 137:194-200. doi:10.1016/j.freeradbiomed.2019.04.035
39. Munzel T, Camici GG, Maack C, Bonetti NR, Fuster V, Kovacic JC (2017) Impact of Oxidative Stress on the Heart and Vasculature: Part 2 of a 3-Part Series. J Am Coll Cardiol 70:212-229. doi:10.1016/j.jacc.2017.05.035
40. Murphy E, Kohr M, Menazza S, Nguyen T, Evangelista A, Sun J, Steenbergen C (2014) Signaling by S-nitrosylation in the heart. J Mol Cell Cardiol 73:18-25. doi:10.1016/j.yjmcc.2014.01.003
41. Murphy MP (2009) How mitochondria produce reactive oxygen species. Biochem J 417:1-13. doi:10.1042/BJ20081386
42. Neubauer S (2007) The failing heart--an engine out of fuel. N Engl J Med 356:1140-1151. doi:10.1056/NEJMra063052
43. Nulton-Persson AC, Szweda LI (2001) Modulation of mitochondrial function by hydrogen peroxide. J Biol Chem 276:23357-23361. doi:10.1074/jbc.M100320200
44. Park JH, Ku HJ, Kim JK, Park JW, Lee JH (2018) Amelioration of High Fructose-Induced Cardiac Hypertrophy by Naringin. Sci Rep 8:2464. doi:10.1038/s41598-018-27788-1
45. Parodi-Rullan RM, Chapa-Dubocq XR, Javadov S (2018) Acetylation of Mitochondrial Proteins in the Heart: The Role of SIRT3. Front Physiol 9:1094. doi:10.3389/fphys.2018.01094
46. Porter GA, Urciuoli WR, Brookes PS, Nadtochiy SM (2014) SIRT3 deficiency exacerbates ischemia-reperfusion injury: implication for aged hearts. Am J Physiol Heart Circ Physiol 306:H1602-1609. doi:10.1152/ajpheart.00027.2014
47. Schieber M, Chandel NS (2014) ROS function in redox signaling and oxidative stress. Curr Biol 24:R453-462. doi:10.1016/j.cub.2014.03.034
48. Sebaa R, Johnson J, Pileggi C, Norgren M, Xuan J, Sai Y, Tong Q, Krystkowiak I, Bondy-Chorney E, Davey NE, Krogan N, Downey M, Harper ME (2019) SIRT3 controls brown fat thermogenesis by deacetylation regulation of pathways upstream of UCP1. Mol Metab 25:35-49. doi:10.1016/j.molmet.2019.04.008
49. Sheeran FL, Pepe S (2016) Posttranslational modifications and dysfunction of mitochondrial enzymes in human heart failure. Am J Physiol Endocrinol Metab 311:E449-460. doi:10.1152/ajpendo.00127.2016
50. Sies H, Jones DP (2020) Reactive oxygen species (ROS) as pleiotropic physiological signalling agents. Nat Rev Mol Cell Biol. doi:10.1038/s41580-020-0230-3
51. Spinazzi M, Casarin A, Pertegato V, Salviati L, Angelini C (2012) Assessment of mitochondrial respiratory chain enzymatic activities on tissues and cultured cells. Nat Protoc 7:1235-1246. doi:10.1038/nprot.2012.058
52. Stram AR, Payne RM (2016) Post-translational modifications in mitochondria: protein signaling in the powerhouse. Cell Mol Life Sci 73:4063-4073. doi:10.1007/s00018-016-2280-4
53. Sundaresan NR, Gupta M, Kim G, Rajamohan SB, Isbatan A, Gupta MP (2009) Sirt3 blocks the cardiac hypertrophic response by augmenting Foxo3a-dependent antioxidant defense mechanisms in mice. J Clin Invest 119:2758-2771. doi:10.1172/JCI39162

54. Sundaresan NR, Samant SA, Pillai VB, Rajamohan SB, Gupta MP (2008) SIRT3 is a stress-responsive deacetylase in cardiomyocytes that protects cells from stress-mediated cell death by deacetylation of Ku70. Mol Cell Biol 28:6384-6401. doi:10.1128/MCB.00426-08
55. Tao R, Coleman MC, Pennington JD, Ozden O, Park SH, Jiang H, Kim HS, Flynn CR, Hill S, Hayes McDonald W, Olivier AK, Spitz DR, Gius D (2010) Sirt3-mediated deacetylation of evolutionarily conserved lysine 122 regulates MnSOD activity in response to stress. Mol Cell 40:893-904. doi:10.1016/j.molcel.2010.12.013
56. Thapa D, Zhang M, Manning JR, Guimaraes DA, Stoner MW, O'Doherty RM, Shiva S, Scott I (2017) Acetylation of mitochondrial proteins by GCN5L1 promotes enhanced fatty acid oxidation in the heart. Am J Physiol Heart Circ Physiol 313:H265-H274. doi:10.1152/ajpheart.00752.2016
57. Varanita T, Soriano ME, Romanello V, Zaglia T, Quintana-Cabrera R, Semenzato M, Menabo R, Costa V, Civiletto G, Pesce P, Viscomi C, Zeviani M, Di Lisa F, Mongillo M, Sandri M, Scorrano L (2015) The OPA1-dependent mitochondrial cristae remodeling pathway controls atrophic, apoptotic, and ischemic tissue damage. Cell Metab 21:834-844. doi:10.1016/j.cmet.2015.05.007
58. Wang SB, Foster DB, Rucker J, O'Rourke B, Kass DA, Van Eyk JE (2011) Redox regulation of mitochondrial ATP synthase: implications for cardiac resynchronization therapy. Circ Res 109:750-757. doi:10.1161/CIRCRESAHA.111.246124
59. Wende AR, Brahma MK, McGinnis GR, Young ME (2017) Metabolic Origins of Heart Failure. JACC Basic Transl Sci 2:297-310. doi:10.1016/j.jacbts.2016.11.009
60. Wittig I, Braun HP, Schagger H (2006) Blue native PAGE. Nat Protoc 1:418-428. doi:10.1038/nprot.2006.62
61. Wu H, Yu Y, David L, Ho YS, Lou MF (2014) Glutaredoxin 2 (Grx2) gene deletion induces early onset of age-dependent cataracts in mice. J Biol Chem 289:36125-36139. doi:10.1074/jbc.M114.620047
62. Yan K, Wang K, Li P (2019) The role of post-translational modifications in cardiac hypertrophy. J Cell Mol Med 23:3795-3807. doi:10.1111/jcmm.14330
63. Yang W, Nagasawa K, Munch C, Xu Y, Satterstrom K, Jeong S, Hayes SD, Jedrychowski MP, Vyas FS, Zaganjor E, Guarani V, Ringel AE, Gygi SP, Harper JW, Haigis MC (2016) Mitochondrial Sirtuin Network Reveals Dynamic SIRT3-Dependent Deacetylation in Response to Membrane Depolarization. Cell 167:985-1000 e1021. doi:10.1016/j.cell.2016.10.016
64. Zhang H, Du Y, Zhang X, Lu J, Holmgren A (2014) Glutaredoxin 2 reduces both thioredoxin 2 and thioredoxin 1 and protects cells from apoptosis induced by auranofin and 4-hydroxynonenal. Antioxid Redox Signal 21:669-681. doi:10.1089/ars.2013.5499
65. Zhang Z, Tan M, Xie Z, Dai L, Chen Y, Zhao Y (2011) Identification of lysine succinylation as a new post-translational modification. Nat Chem Biol 7:58-63. doi:10.1038/nchembio.495
66. Zhu H, Sun A (2018) Programmed necrosis in heart disease: Molecular mechanisms and clinical implications. J Mol Cell Cardiol 116:125-134. doi:10.1016/j.yjmcc.2018.01.018
67. Zorov DB, Juhaszova M, Sollott SJ (2006) Mitochondrial ROS-induced ROS release: an update and review. Biochim Biophys Acta 1757:509-517. doi:10.1016/j.bbabio.2006.04.029

Credit Author statement:

MEH conceived the idea for the project. NTB, BM, and CP performed all experiments to assess mitochondrial function, and NTB analyzed the data. BM performed immunoblotting. CP and GP performed immunoblotting, glutathione analyses and respiratory complex activity. BM acquired the human data from GTEx consortium, and the data was analyzed by BM and KM. NTB and MEH wrote the paper and all authors reviewed and approved it.

Declaration of interests

☒ The authors declare that they have no known competing financial interests or personal relationships that could have appeared to influence the work reported in this paper.

☐The authors declare the following financial interests/personal relationships which may be considered as potential competing interests:

Highlights

- GRX2 and SIRT3 are important in the control of oxidative stress and mitochondrial function in the heart
- The absence of both GRX2 and SIRT3 impairs overall mitochondrial respiratory capacity
- In human left ventricle tissue, expression of GRX2 and SIRT3 is positively correlated